Electroreduction of CO on Polycrystalline Copper at Low Overpotentials

Bertheussen, Erlend; Vagn Hogg, Thomas; Abghoui, Younes; Engstfeld, Albert Kilian; Chorkendorff, Ib; Stephens, Ifan E. L.

Published in:
ACS Energy Letters

Link to article, DOI:
10.1021/acsenergylett.8b00092

Publication date:
2018

Document Version
Peer reviewed version

Electroreduction of CO on Polycrystalline Copper at Low Overpotentials

Erlend Bertheussen[¶,†], *Thomas V. Hogg*[¶,†], *Younes Abghoui*[†,‡], *Albert K. Engstfeld*[†,§], *Ib Chorkendorff*[*,†], *Ifan E. L. Stephens*[*,†,||]

[†]Section for Surface Physics and Catalysis, Department of Physics, Technical University of Denmark, DK-2800 Kgs. Lyngby, Denmark;

[‡]Science Institute and Faculty of Physical Sciences, VR-III, University of Iceland, IS-107 Reykjavik, Iceland;

[§]Institute of Surface Chemistry and Catalysis, Ulm University, D-89069 Ulm, Germany

[||]Department of Materials, Imperial College London, Royal School of Mines, London, SW7 2AZ, UK.

Corresponding Authors

* E-mail: ibchork@fysik.dtu.dk (I.C.)

E-mail: i.stephens@imperial.ac.uk (I.E.L.S.)

ABSTRACT: Cu is the only monometallic electrocatalyst to produce highly reduced products from CO_2 selectively due to its intermediate binding of CO. We investigate the performance of polycrystalline Cu for the electroreduction of CO in alkaline media (0.1 M KOH) at low overpotentials (-0.4 to -0.6 V vs RHE). We find that polycrystalline Cu is highly active at these potentials. The overall CO reduction rates are comparable to nanostructured forms of the material, albeit with a distinct product distribution. While nanostructured forms of Cu favor alcohols, polycrystalline Cu produces greater amounts of C_2 and C_3 aldehydes, as well as ethylene.

TOC GRAPHICS

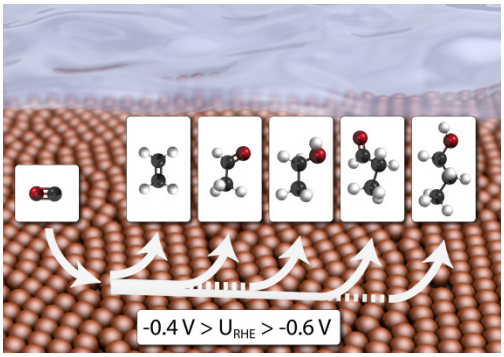

Electrochemical reduction using renewable energy is emerging as a promising mean of recycling carbon dioxide (CO_2) from point sources or ambient air into useful chemicals.[1–3] This way, the anthropogenic carbon cycle can be closed and our dependence on fossil energy sources to produce fuels and commodity chemicals can be reduced. The successful implementation of this technology requires development of electrocatalysts that can produce the desired product(s) efficiently and selectively.[1,2] Examples of useful products are energy-rich compounds such as hydrocarbons and oxygenates that can be used either as fuels or commodity chemicals.[1] Multi-carbon (C_{2+}) products are of special interest, due to their high energy density.[4] Moreover, unlike C_1 products such as methanol, they are particularly challenging to synthesize via thermally activated CO or CO_2 reduction methods.[5]

Copper is the only pure metal that can convert CO_2 into highly reduced and C-C coupled products in significant amounts.[6,7] This process, however, requires large overpotentials, and a large number of compounds are produced. In order to make this process suitable for large scale energy conversion, significant improvements are necessary. One approach is to use a tandem system whereby CO_2 is reduced in two stages: (i) reduce CO_2 to CO followed by (ii) further reduction of CO to more energy-rich products.[8] Several catalysts, including nanostructured Au,[9–11] Ag[12] and transition metal doped, nitrogenated carbon,[13–15] are highly selective and moderately active for the first step. For the second step, Cu based materials are the only catalysts to reduce CO at significant rates and with reasonable selectivity.[16] In particular, works led by Hori[16] and Koper[17] showed that C_2 products are favored under more alkaline conditions; subsequent theoretical works suggested that C-C coupling barriers are lower at high pH.[18,19] Moreover, increased surface roughness generally seems to favor the production of C_2 products, such as ethylene from CO_2.[20–24] Here, it is worth pointing out the significant difference in performance between aqueous half-cell measurements and experiments performed in real devices.[1] In aqueous electrolytes, CO_2 and CO reduction is limited by the low solubility of the reactant gas.[4] One

means of dealing with this issue is to conduct experiments on gas diffusion electrodes, which are not completely submerged in the electrolyte.[25,26]

Building upon the earlier findings regarding CO reduction on Cu electrodes, Kanan and co-workers showed that oxide-derived, nanostructured copper has a high (geometrically normalized) activity towards CO reduction at low overpotentials in 0.1 M KOH.[8] It exhibited high selectivity towards ethanol, with a maximum Faradaic efficiency of 43% at -0.3 V vs. RHE. The authors attributed the activity to a high density of grain boundary surface terminations.[8,27] A study from our own laboratory showed that the CO evolution activity was strongly correlated to the presence of a site – presumably undercoordinated – with exceptionally strong interaction with CO.[28] Other groups have also reported that stepped or kinked surfaces yield higher proportions of oxygenates, relative to hydrocarbons, from CO_2 or CO reduction.[29–31] This phenomenon is likely related to the more favorable free energy pathway for aldehyde reduction to alcohols on high index Cu surfaces than on terraces.[32]

Oxide derived-Cu evidently has a complex surface chemistry;[27,28] moreover its porous morphology is likely to yield mesoscopic transport effects during CO reduction, especially given the involvement of soluble intermediates such as acetaldehyde.[33–35] On the other hand, the chemistry of CO reduction on polycrystalline Cu should be simpler; on that basis, it could be used as a robust benchmark for activity measurements. To the best of our knowledge, there are only two reports in the literature that quantify the activity and selectivity of planar polycrystalline Cu for CO reduction in 0.1 M KOH.[28,36] Even so, there is significant variability between those two reports, as described in more detail in the supporting information (Section S3 and Figure S1). This leads us to the focus of the current investigation, which is to establish the following: *What is the activity of polycrystalline Cu for CO reduction, a viable benchmark for this reaction on copper based electrodes? How does it compare in terms of activity and Faradaic efficiency to literature data on nanostructured copper materials?* On the basis of our current understanding, we aim to establish the reasons for the fundamental differences in

catalytic performance between polycrystalline and nanostructured Cu. Consequently, we investigate CO reduction on polycrystalline copper foils between -0.40 V and -0.59 V vs. RHE , i.e. at potentials more positive than previously reported for this material. We report appreciable activity and selectivity to CO reduction across this potential range. We also show that the total CO reduction current density of polycrystalline copper is comparable to that of oxide-derived copper, when normalized to electrochemical surface area (ECSA).

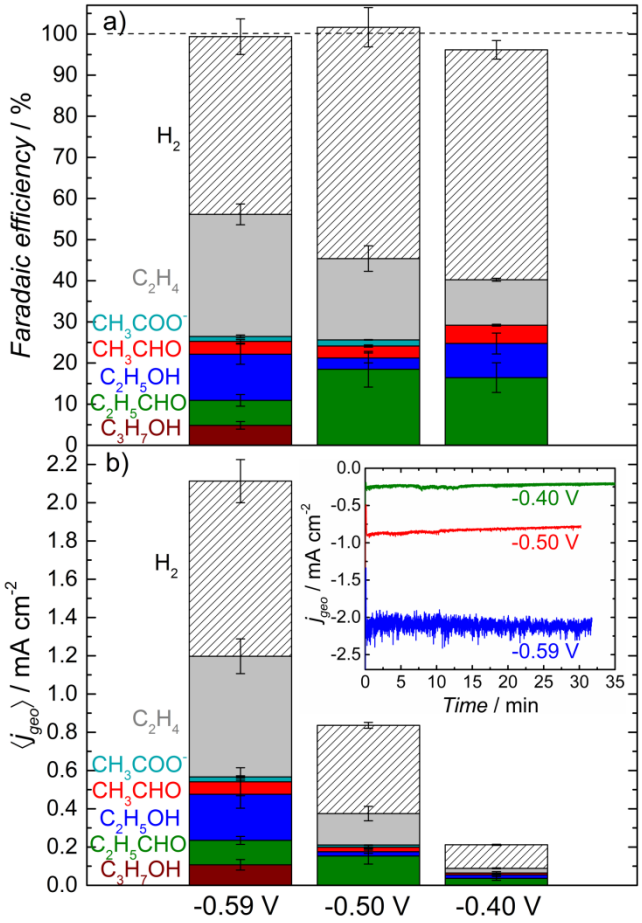

Figure 1. Faradaic efficiency (a) and mean partial current density (b) from chronoamperometric CO reduction performed in CO saturated 0.1 M KOH at -0.40, -0.50 and -0.59 V vs. RHE. Data represent the average of 3 individual measurements, and error bars indicate ±σ. Inset: Chronoamperometry traces from representative measurements at each potential. Measurements were carried out until a certain charge was reached (0.5 C at -0.40 V, 1.5 C at -0.50 V and 4.0 C at -0.59 V).

Acivity and product distribution from CO reduction on polycrystalline Cu. We carried out short-term (~30 minutes) chronoamperometric CO reduction measurements at three different potentials, i.e., -0.40, -0.50 and -0.59 V vs. RHE (all potentials are referred to this scale in the following) in CO-saturated 0.1 M KOH electrolyte using a glass H-cell. The resulting Faradaic efficiencies and partial current densities for the individual products are shown in Figure 1a and 1b, respectively. Within the uncertainty of our measurements, we could account for a 100% balance of charge with products detected, including both H_2 and compounds derived from CO reduction. We observed that the Faradaic efficiency towards CO reduction increases from 40% at -0.40 V to 56% at -0.59 V. Consistent with earlier reports on oxide-derived Cu,[8,27,28,33] only C_{2+} products are formed under these conditions. The two major CO reduction products are propionaldehyde (with a maximum of 18% Faradaic efficiency at -0.50 V) and ethylene (30% at -0.59 V). The other CO reduction products are ethanol, 1-propanol, acetaldehyde and acetate. The rates towards alcohol production are particularly high at the most negative potential, -0.59 V where the concentration of 1-propanol exceeds the detection limit of our analytical equipment. Notably, we measured significant CO reduction partial current densities, up to 1.2 mA cm^{-2} at -0.59 V.

Another important observation is how the product distribution changes with the applied potential. Among the oxygenated compounds, aldehydes are formed primarily at the more positive potentials, while alcohol formation becomes more prominent at -0.59 V. Several studies, including results from our group, show that acetaldehyde is an intermediate in the production of ethanol.[16,32,33] Hori et al. reported that propionaldehyde could be reduced to 1-propanol on polycrystalline copper strongly suggesting that also the C_3 aldehyde is an intermediate in alcohol formation.[16] It seems that applying -0.59 V instead of -0.50 V accelerates aldehyde conversion to alcohols. It is worth noting that aldehydes are challenging to

detect in alkaline solutions using routine NMR spectroscopy.[33,37] However, our use of static headspace-gas chromatography (HS-GC) enables us to measure these compounds with high sensitivity.

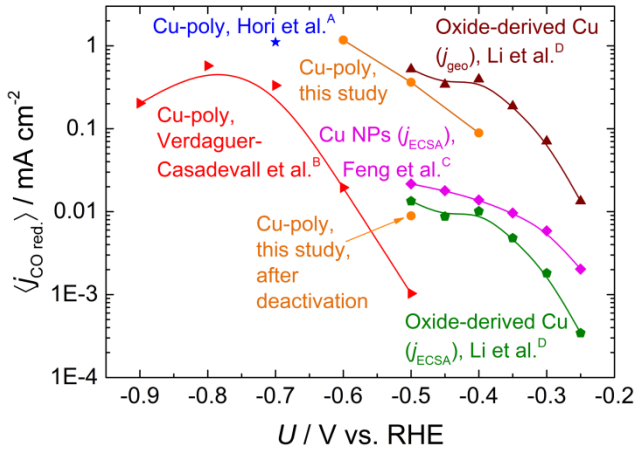

Figure 2. Comparison of mean partial current densities for CO reduction on polycrystalline Cu, oxide derived Cu and Cu nanoparticles. Oxide derived Cu is normalized with respect to both geometric and electrochemically active surface area. The results from the current study are the same that are shown in Figure 1, and are compared with data adapted from (A) Hori et al.,[36] (B) Verdaguer-Casadevall et al.,[28] (C) Feng et al.[27] and (D) Li et al.[8] The bottom orange point represents the result from a sample after deactivation, for which detailed data are shown in Figure S2. We have summarized the roughness factors we used for the ECSA normalization in Table S2, obtained from each of the relevant studies. We assume that the polycrystalline Cu electrodes have a roughness factor of 1.

Comparison with literature data for polycrystalline Cu and nanostructured Cu. Figure 2 compares the total CO reduction current densities of this work with some results from relevant studies reported in the literature. An interesting comparison can be drawn between the results from this work and previously published data from oxide-derived Cu and Cu nanoparticles. It seems that nanostructured electrodes reach mass transport limitations for CO reduction at potentials just cathodic of -0.30 V to -

0.35 V. By extrapolating the first two to three points of the data that are normalized to electrochemical surface area (ECSA) , it seems that these lines would roughly coincide with the polycrystalline data from the present work. This suggests that the activity towards CO reduction for nanostructured copper is actually similar to that of polycrystalline copper. Thus, according to our data, there is no significant difference between the CO reduction activity of planar polycrystalline Cu and nanostructured oxide derived Cu: the high current densities of the oxide derived Cu – when normalized to geometric surface area – are due to the exceptionally large roughness factors of 39 or higher. This important observation shows that nanostructuring is not a prerequisite for high CO reduction activity.

There are significant variations in product distribution between the two types of materials. An example of this is the difference in ethylene production. Polycrystalline copper shows significant selectivity to ethylene at all potentials measured in this study, in particular at -0.5 V and more cathodic. On nanostructured copper, on the other hand, ethylene is not produced in significant amounts, probably because these catalysts are mass transport limited in the region where hydrocarbons are normally produced.

At the same time, oxygenates are almost exclusively produced from CO reduction on nanostructured electrodes when not mass transport limited. It has been shown for CO_2 reduction that oxygenates are generally produced at lower overpotentials than hydrocarbons.[38] This points towards the different potential regions accessible on planar and nanostructured surfaces as a likely reason for the variation in oxygenate selectivity. The high ECSA of the nanostructured electrodes allows for measurements at lower overpotentials, since the larger geometric current density allows for adequate product analysis even though the ECSA-normalized current density is low. On the other hand, such electrodes reach mass transport limitations already around -0.35 V, as discussed above. As a result, the potential range accessible to measurements is distinct from planar electrodes. It is also evident that nanostructured oxide derived Cu yields higher selectivity to energy-rich alcohols than planar

polycrystalline Cu.[8,33] We attribute this phenomenon to two effects: (i) oxide-derived Cu has more strong-binding undercoordinated sites, which are more effective at reducing aldehydes to alcohols, as discussed in the introduction, and (ii) the porosity leads to enhanced retention of aldehydes, accelerating their reduction to alcohols. We would like to emphasise that the low ECSA of polycrystalline Cu makes it an unsuitable CO reduction catalyst for commercial purposes. However, we consider it provides an excellent, simple-to-reproduce benchmark. Moreover, it is of critical interest to establish the differences between it and nanostructured forms of Cu in order to design improved catalyst materials.

When comparing the individual studies on polycrystalline copper, it can be seen that they differ significantly from each other. For instance, our present results show significant CO reduction activity for polycrystalline copper between -0.40 V and -0.59 V, whereas the results of an earlier collaboration between our group and Kanan and coworkers showed little to no CO reduction activity at potentials between -0.50 and -0.90 V on similar electrodes.[28] We speculate that these differences could be caused, at least partly, by the longer duration of the measurements in that study. They were carried out for 2-3 hours, a period in which the electrodes in the current study experience significant deactivation. We mainly attribute this deactivation to poisoning by silicon from the glassware, as discussed in detail below. In Figure 2, we show a data point from a measurement carried out on an electrode that had already been deactivated in argon-purged electrolyte (chronoamperometry trace and Faradaic efficiency are shown in Figure S2). Its activity is much closer to the data from Verdaguer-Casadevall et al., suggesting that those data could have been affected by silicon poisoning. In addition to the studies mentioned above, Koper and coworkers also investigated CO reduction on polycrystalline Cu. They observe formation of ethylene between -0.35 and -0.60 V on polycrystalline Cu, but with insignificant overall current densities.4 The authors use online electrochemical mass spectrometry (OLEMS) for product analysis: this technique is highly sensitive to gas phase species; however, it is challenging to use

it to yield quantitative measurements of reaction rates. On that basis, we have not included it in Figure 2.

In general, the low ECSA of planar electrodes makes them far more susceptible to poisoning by impurities than their nanostructured counterparts with a more favorable electrode area/electrolyte volume ratio. When studying the intrinsic behavior of low surface area electrocatalysts, we recommend keeping the measurement time as short as possible, so that the effect of any impurities that might be present is minimized. For CO_2/CO reduction measurements, the measurement duration is normally limited by accumulation of liquid products above the detection limits of the analytical equipment used.

Another reason for the discrepancies could be differences in initial electrode surface structure. In Figure S3, we show that different batches of copper foils from the same supplier can give significantly different features in CVs under inert gas conditions. This is reflected in the CO reduction activity shown in Figure S4, where the foil that exhibits more (100)-like features shows higher CO reduction selectivity, in particular towards ethylene formation. Several groups have shown that the surface orientation of copper electrocatalysts can have a significant effect on CO reduction performance.[29–31,39–42] Thus, we conjecture that the surface orientation of different polycrystalline foils could also vary significantly, hence affecting the catalyst activity.

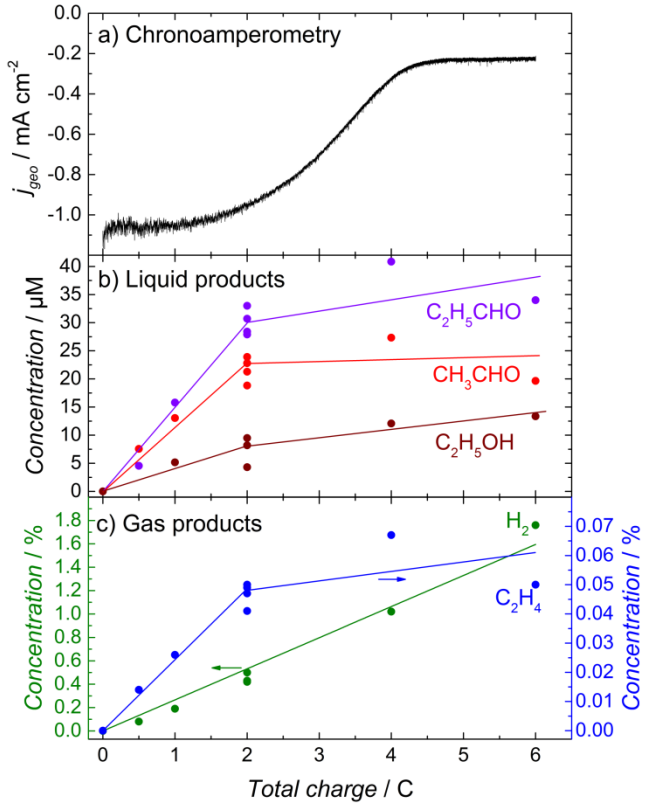

Figure 3. CO reduction measurements at -0.52 V in CO saturated 0.1 M KOH. (a) Chronoamperometry trace for measurement stopped at 6 C charge. (b) Concentration of the liquid products ethanol, acetaldehyde and propionaldehyde as a function of total measurement charge. (c) Concentration of the individual gaseous products as a function of total measurement charge. Note: 1-propanol and acetate are not shown in (b). 1-propanol was not produced in concentrations above our detection limits at this potential, and acetate was measured using NMR spectroscopy, which was not carried out for these measurements. Acetate is a minor product quantified to ~1% Faradaic efficiency in other measurements. Each data point in (b) and (c) represents data from an individual measurement. Lines have been added to guide the eye. The corresponding duration of each measurement is shown in Figure S6b in the Supporting Information.

Deactivation for extended measurements. Using our current experimental setup, it is challenging to maintain the activity of Cu for extended periods of time. Representative chronoamperometry traces

for short-term measurements are shown in the inset of Figure 1b. The high CO reduction activity that we described above is relatively stable over the course of ~30 minutes at all three potentials. A minor loss of activity can be observed at -0.40 V and -0.50 V, while the measurements at -0.59 V are completely stable. Significant deactivation occurs on a longer time scale, however (current density as a function of time for the same measurement is shown in Figure S5, total CO reduction partial current density for each point is shown in Figure S6b). For the measurement shown in Figure 3a, the initial current density decreases by almost 80%. At the same time, a strong shift in product distribution can be observed. In Figure 3b and c, the development of product concentration with total measurement charge is shown for liquid and gaseous products, respectively. The H_2 concentration increases linearly with accumulated measurement charge. On the other hand, at the point where the current density starts rapidly decreasing, the concentration of the CO reduction products ethylene, acetaldehyde, propionaldehyde and ethanol reaches a plateau. The slope of the H_2 concentration would, in principle, be expected to increase when deactivation starts, due to an increase in Faradaic efficiency. A minor leakage of H_2 for measurements longer than ~30 minutes could be the reason that this is not the case.

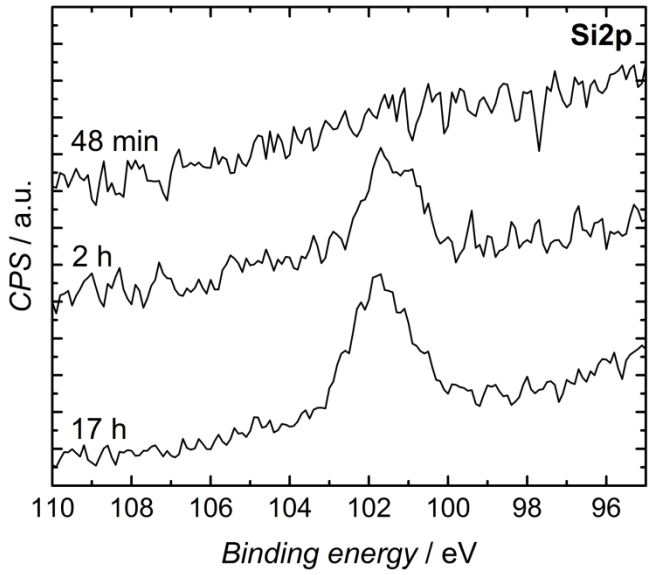

Figure 4. XPS spectra of the Si2p binding energy region on polycrystalline copper foils after CO reduction at -0.50 V for different times. Note: Each measurement is carried out on a new CO reduction sample.

The observed catalyst deactivation could be caused by several effects, including i) changes in the elemental composition of the surface due to accumulation of impurities,[43–47] ii) the electropolished Cu surface undergoing a structural transformation under reaction conditions,[30,39,48] and/or iii) self-poisoning of the surface by reaction products/intermediates, as shown previously for other reactions, e.g., by Heinen et al. for the electrooxidation of ethanol.[34] In order to investigate possible impurity deposition of the electrode, we performed X-ray photoelectron spectroscopy (XPS) studies after the CO reduction measurement. In Figure 4, we show XPS spectra of the Si2p region measured on copper electrodes after different electrolysis times. For short-term measurements, where significant deactivation has not yet occurred, little or no Si can be detected on the surface with this technique. For longer measurements, however, the Si2p line is clearly visible, suggesting that there might be a correlation between the presence of Si and the deactivation. Mayrhofer et al. showed that Pb and Si, derived from glass corrosion under alkaline conditions, can poison reactions such as O_2 reduction on Pt.[43,44] Since we are using glass cells for these measurements, it is a plausible reason for the deactivation we see. Figure S7 shows a survey spectrum of an electrode after long-term CO reduction. No clear lines of other possible metallic contaminants are present.

To investigate whether self-poisoning by aldehydes contribute to the observed deactivation, we added acetaldehyde and propionaldehyde to Ar-saturated 0.1 M KOH and carried out chronoamperometry measurements at -0.50 V. We chose aldehydes for this measurement as a result of our previous observation that acetaldehyde undergoes spontaneous organic reactions in alkaline solution, including polymerization.[33] The resulting trace is displayed in Figure S8. Initially, an increased current density can be observed, suggesting that the aldehydes do not immediately poison the surface.

The electrode does, however start losing activity after ~30 minutes, similarly to the long-term CO reduction measurement shown in Figure S5. In order to elucidate if restructuring of the electrode under reaction conditions occurs, and influences the activity, we also investigated the behavior of the electrode when kept at -0.50 V in Ar-purged electrolyte, before switching to CO. The resulting chronoamperometry trace and the respective product distribution are shown in Figure S2. After an initial activation, the H_2 evolution current starts to deactivate as well. After switching to CO, the initial activity is significantly lower than right after electropolishing. Furthermore, only small amounts of CO reduction products could be detected. These experiments together suggest that self-poisoning by reaction intermediates is not causing the deactivation. They do not, however, conclusively show if silicon poisoning or restructuring are causing it, or a combination of both effects.

In this study, we investigated the activity and product selectivity of polycrystalline Cu for the reduction of CO at low overpotentials in alkaline media. We measured more than 50% Faradaic efficiency for CO reduction, primarily due to the formation of C_2 and C_3 aldehydes and alcohols, as well as ethylene. A comparison of data from this study with results reported previously in the literature indicates that polycrystalline Cu can yield comparable CO reduction rates to oxide-derived, nanostructured Cu. Even so, oxide-derived Cu favors the production of highly-coveted energy-rich alcohols; we attribute this difference to a higher abundance of undercoordinated sites and decreased mass transport within the pores of oxide derived Cu. In summary, by performing bulk electrolysis measurements using three different analytical chemistry techniques, we demonstrate that planar polycrystalline copper exhibits equivalent activity for CO reduction to state-of-the-art nanostructured catalyst materials. The enhanced current densities afforded by nanostructured surfaces are only due to the large surface area. Future studies should focus on improving the *intrinsic activity* of Cu.

EXPERIMENTAL DETAILS

A more detailed description of materials used (Section S1) and experimental details (Section S2) can be found in the Supporting Information.

Polycrystalline copper electrodes were cut to a size of 5x10 mm, and a piece of copper wire was attached. The electrodes were electropolished in 30% phosphoric acid and rinsed thoroughly with MilliQ water. The procedure was carried out immediately before the electrode was mounted in the custom made H-cell. The electrolyte was purged with CO for 15 minutes at 30 sccm. The ohmic resistance was measured using electrochemical impedance spectroscopy. 85% of the Ohmic drop was compensated for in the EC-Lab software, with post-measurement correction applied to account for the final 15%. A Hg/Hg_2SO_4 reference electrode was used for all measurements, converted into the RHE scale by calibration against the onset of H_2 evolution/H_2 oxidation on a Pt electrode. CO reduction was carried out in batch measurements. Chronoamperometry was carried out until a certain amount of charge was passed. For short-term measurements the values for total measurement charge were 0.5 C at -0.40 V, 1.5 C at -0.50 V and 4.0 C at -0.59 V. The average current from a measurement was used in later analyses. After chronoamperometry, 250 μL of the gas mixture was injected in the GC. Liquid product analysis was performed using HS-GC and NMR spectroscopy following the protocols from a previous publication.[37] XPS was performed using an Al Kα X-ray source. An Ar flood gun was used for sample charge neutralization.

ASSOCIATED CONTENT

Supporting Information

The Supporting Information is available free of charge on the ACS Publications website at DOI: XXXX

Materials; detailed experimental methods; existing literature regarding CO reduction on polycrystalline Cu; pre-reduction in Ar; roughness factors; cyclic voltammograms and product distribution measured on two different batches of Cu foils; chronoamperometry trace and charge

dependence of long-term measurements; XPS survey spectrum; aldehyde reduction; tabulated values for CO reduction activity and product distribution.

AUTHOR INFORMATION

Corresponding Authors

* E-mail: ibchork@fysik.dtu.dk (I.C.)

* E-mail: i.stephens@imperial.ac.uk (I.E.L.S.)

Author Contributions

¶E.B. and T.V.H. contributed equally to this work.

Present Addresses

‡ Y.A.: Science Institute, Faculty of Physical Sciences, VR-III, University of Iceland, IS-107 Reykjavik, Iceland

§ A.K.E.: Institute of Surface Chemistry and Catalysis, Ulm University, D-89069 Ulm, Germany

|| I.E.L.S.: Department of Materials, Imperial College London, Royal School of Mines, London, SW7 2AZ, UK.

ACKNOWLEDGMENTS

This work was funded by the Villum Foundation V-SUSTAIN grant 9455 to the Villum Center for the Science of Sustainable Fuels and Chemicals.

Y.A received funding from The Icelandic Research Fund;

A.K.E. received funding from the People Program (Marie Curie Actions) of the European Union's Seventh Framework Program (FP7/2007-2013) under REA grant agreement n°609405 (COFUNDPostdocDTU).*info on website

We thank Jakob Kibsgaard for producing the table of content graphic.

REFERENCES

(1) Whipple, D. T.; Kenis, P. J. A. Prospects of CO_2 Utilization via Direct Heterogeneous Electrochemical Reduction. *J. Phys. Chem. Lett.* **2010**, *1*, 3451–3458.

(2) Seh, Z. W.; Kibsgaard, J.; Dickens, C. F.; Chorkendorff, I.; Nørskov, J. K.; Jaramillo, T. F. Combining Theory and Experiment in Electrocatalysis: Insights into Materials Design. *Science* **2017**, *355*, 1–12.

(3) Hori, Y. Electrochemical CO_2 Reduction on Metal Electrodes. In *Modern Aspects of Electrochemistry*; Vayenas, C. G., White, R. E., Gamboa-Aldeco, M. E., Eds.; Springer, 2008; Vol. 42, pp 89–189.

(4) *CRC Handbook of Chemistry and Physics*, 97th ed.; Haynes, W. M., Ed.; CRC Press/Taylor & Francis: Boca Raton, FL, 2016.

(5) Medford, A. J.; Lausche, A. C.; Abild-Pedersen, F.; Temel, B.; Schjødt, N. C.; Nørskov, J. K.; Studt, F. Activity and Selectivity Trends in Synthesis Gas Conversion to Higher Alcohols. *Top. Catal.* **2014**, *57*, 135–142.

(6) Hori, Y.; Wakebe, H.; Tsukamoto, T.; Koga, O. Electrocatalytic Process of CO Selectivity in Electrochemical Reduction of CO_2 at Metal Electrodes in Aqueous Media. *Electrochim. Acta* **1994**, *39*, 1833–1839.

(7) Bagger, A.; Ju, W.; Varela, A. S.; Strasser, P.; Rossmeisl, J. Electrochemical CO_2 Reduction: A Classification Problem. *ChemPhysChem* **2017**, *18*, 3266–3273.

(8) Li, C. W.; Ciston, J.; Kanan, M. W. Electroreduction of Carbon Monoxide to Liquid Fuel on Oxide-Derived Nanocrystalline Copper. *Nature* **2014**, *508*, 504–507.

(9) Zhu, W.; Michalsky, R.; Metin, Ö.; Lv, H.; Guo, S.; Wright, C. J.; Sun, X.; Peterson, A. A.; Sun,

S. Monodisperse Au Nanoparticles for Selective Electrocatalytic Reduction of CO_2 to CO. *J. Am. Chem. Soc.* **2013**, *135*, 16833–16836.

(10) Zhu, W.; Zhang, Y.-J.; Zhang, H.; Lv, H.; Li, Q.; Michalsky, R.; Peterson, A. A.; Sun, S. Active and Selective Conversion of CO_2 to CO on Ultrathin Au Nanowires. *J. Am. Chem. Soc.* **2014**, *136*, 16132–16135.

(11) Chen, Y.; Li, C. W.; Kanan, M. W. Aqueous CO_2 Reduction at Very Low Overpotential on Oxide-Derived Au Nanoparticles. *J. Am. Chem. Soc.* **2012**, *134*, 19969–19972.

(12) Mistry, H.; Choi, Y.-W.; Bagger, A.; Scholten, F.; Bonifacio, C. S.; Sinev, I.; Divins, N. J.; Zegkinoglou, I.; Jeon, H. S.; Kisslinger, K.; et al. Enhanced Carbon Dioxide Electroreduction to Carbon Monoxide over Defect-Rich Plasma-Activated Silver Catalysts. *Angew. Chem. Int. Ed.* **2017**, *56*, 11394–11398.

(13) Varela, A. S.; Ranjbar Sahraie, N.; Steinberg, J.; Ju, W.; Oh, H. S.; Strasser, P. Metal-Doped Nitrogenated Carbon as an Efficient Catalyst for Direct CO_2 Electroreduction to CO and Hydrocarbons. *Angew. Chem. Int. Ed.* **2015**, *54*, 10758–10762.

(14) Bagger, A.; Ju, W.; Varela, A. S.; Strasser, P.; Rossmeisl, J. Single Site Porphyrine-Like Structures Advantages over Metals for Selective Electrochemical CO_2 reduction. *Catal. Today* **2017**, *288*, 74–78.

(15) Ju, W.; Bagger, A.; Hao, G. P.; Varela, A. S.; Sinev, I.; Bon, V.; Roldan Cuenya, B.; Kaskel, S.; Rossmeisl, J.; Strasser, P. Understanding Activity and Selectivity of Metal-Nitrogen-Doped Carbon Catalysts for Electrochemical Reduction of CO_2. *Nat. Commun.* **2017**, *8*, 944.

(16) Hori, Y.; Takahashi, R.; Yoshinami, Y.; Murata, A. Electrochemical Reduction of CO at a Copper Electrode. *J. Phys. Chem. B* **1997**, *101*, 7075–7081.

(17) Schouten, K. J. P.; Kwon, Y.; van der Ham, C. J. M.; Qin, Z.; Koper, M. T. M. A New Mechanism for the Selectivity to C_1 and C_2 Species in the Electrochemical Reduction of Carbon Dioxide on Copper Electrodes. *Chem. Sci.* **2011**, *2*, 1902.

(18) Calle-Vallejo, F.; Koper, M. T. M. Theoretical Considerations on the Electroreduction of CO to C_2 Species on Cu(100) Electrodes. *Angew. Chem. Int. Ed.* **2013**, *52*, 7282–7285.

(19) Montoya, J. H.; Shi, C.; Chan, K.; Nørskov, J. K. Theoretical Insights into a CO Dimerization Mechanism in CO_2 Electroreduction. *J. Phys. Chem. Lett.* **2015**, *6*, 2032–2037.

(20) Tang, W.; Peterson, A. A.; Varela, A. S.; Jovanov, Z. P.; Bech, L.; Durand, W. J.; Dahl, S.; Nørskov, J. K.; Chorkendorff, I. The Importance of Surface Morphology in Controlling the Selectivity of Polycrystalline Copper for CO_2 Electroreduction. *Phys. Chem. Chem. Phys.* **2012**, *14*, 76–81.

(21) Roberts, F. S.; Kuhl, K. P.; Nilsson, A. High Selectivity for Ethylene from Carbon Dioxide Reduction over Copper Nanocube Electrocatalysts. *Angew. Chem. Int. Ed.* **2015**, *54*, 5179–5182.

(22) Mistry, H.; Varela, A. S.; Bonifacio, C. S.; Zegkinoglou, I.; Sinev, I.; Choi, Y.-W.; Kisslinger, K.; Stach, E. A.; Yang, J. C.; Strasser, P.; et al. Highly Selective Plasma-Activated Copper Catalysts for Carbon Dioxide Reduction To Ethylene. *Nat. Commun.* **2016**, *7*, 1–8.

(23) Kim, D.; Lee, S.; Ocon, J. D.; Jeong, B.; Lee, J. K.; Lee, J. Insights into an Autonomously Formed Oxygen-Evacuated Cu_2O Electrode for the Selective Production of C_2H_4 from CO_2. *Phys. Chem. Chem. Phys.* **2014**, *17*, 824–830.

(24) Ren, D.; Deng, Y.; Handoko, A. D.; Chen, C. S.; Malkhandi, S.; Yeo, B. S. Selective Electrochemical Reduction of Carbon Dioxide to Ethylene and Ethanol on Copper(I) Oxide Catalysts. *ACS Catal.* **2015**, *5*, 2814–2821.

(25) Ma, S.; Sadakiyo, M.; Luo, R.; Heima, M.; Yamauchi, M.; Kenis, P. J. A. One-Step Electrosynthesis of Ethylene and Ethanol from CO_2 in an Alkaline Electrolyzer. *J. Power Sources* **2016**, *301*, 219–228.

(26) Reller, C.; Krause, R.; Volkova, E.; Schmid, B.; Neubauer, S.; Rucki, A.; Schuster, M.; Schmid, G. Selective Electroreduction of CO_2 toward Ethylene on Nano Dendritic Copper Catalysts at High Current Density. *Adv. Energy Mater.* **2017**, *7*, 1602114.

(27) Feng, X.; Jiang, K.; Fan, S.; Kanan, M. W. A Direct Grain-Boundary-Activity Correlation for CO Electroreduction on Cu Nanoparticles. *ACS Cent. Sci.* **2016**, *2*, 169–174.

(28) Verdaguer-Casadevall, A.; Li, C. W.; Johansson, T. P.; Scott, S. B.; McKeown, J. T.; Kumar, M.; Stephens, I. E. L.; Kanan, M. W.; Chorkendorff, I. Probing the Active Surface Sites for CO Reduction on Oxide-Derived Copper Electrocatalysts. *J. Am. Chem. Soc.* **2015**, *137*, 9808–9811.

(29) Hori, Y.; Takahashi, I.; Koga, O.; Hoshi, N. Electrochemical Reduction of Carbon Dioxide at Various Series of Copper Single Crystal Electrodes. *J. Mol. Catal. A Chem.* **2003**, *199*, 39–47.

(30) Kim, Y. G.; Javier, A.; Baricuatro, J. H.; Soriaga, M. P. Regulating the Product Distribution of CO Reduction by the Atomic-Level Structural Modification of the Cu Electrode Surface. *Electrocatalysis* **2016**, *7*, 391–399.

(31) Hahn, C.; Hatsukade, T.; Kim, Y. G.; Vailionis, A.; Baricuatro, J. H.; Higgins, D. C.; Nitopi, S. A.; Soriaga, M. P.; Jaramillo, T. F. Engineering Cu surfaces for the electrocatalytic conversion of CO_2: Controlling selectivity toward oxygenates and hydrocarbons. *Proc. Natl. Acad. Sci. U. S. A.* **2017**, *114*, 5918–5923.

(32) Ledezma-Yanez, I.; Gallent, E. P.; Koper, M. T. M.; Calle-Vallejo, F. Structure-Sensitive Electroreduction of Acetaldehyde to Ethanol on Copper and its Mechanistic Implications for CO

and CO_2 reduction. *Catal. Today* **2016**, *262*, 90–94.

(33) Bertheussen, E.; Verdaguer-Casadevall, A.; Ravasio, D.; Montoya, J. H.; Trimarco, D. B.; Roy, C.; Meier, S.; Wendland, J.; Nørskov, J. K.; Stephens, I. E. L.; et al. Acetaldehyde as an Intermediate in the Electroreduction of Carbon Monoxide to Ethanol on Oxide-Derived Copper. *Angew. Chem. Int. Ed.* **2016**, *55*, 1450–1454.

(34) Heinen, M.; Jusys, Z.; Behm, R. J. Ethanol, Acetaldehyde and Acetic Acid Adsorption/Electrooxidation on a Pt Thin Film Electrode: An in Situ ATR-FTIRS Flow-Cell Study. *J. Phys. Chem. C* **2010**, *114*, 9850–9864.

(35) Hall, A. S.; Yoon, Y.; Wuttig, A.; Surendranath, Y. Mesostructure-Induced Selectivity in CO_2 Reduction Catalysis. *J. Am. Chem. Soc.* **2015**, *137*, 14834–14837.

(36) Hori, Y.; Murata, A.; Takahashi, R.; Suzuki, S. Electroreduction of CO to CH_4 and C_2H_4 at a Copper Electrode in Aqueous Solutions at Ambient Temperature and Pressure. *J. Am. Chem. Soc.* **1987**, *109*, 5022–5023.

(37) Bertheussen, E.; Abghoui, Y.; Jovanov, Z. P.; Varela, A. S.; Stephens, I. E. L.; Chorkendorff, I. Quantification of Liquid Products from the Electroreduction of CO_2 and CO using Static Headspace-Gas Chromatography and Nuclear Magnetic Resonance Spectroscopy. *Catal. Today* **2017**, *288*, 54–62.

(38) Kuhl, K. P.; Cave, E. R.; Abram, D. N.; Jaramillo, T. F. New Insights into the Electrochemical Reduction of Carbon Dioxide on Metallic Copper Surfaces. *Energy Environ. Sci.* **2012**, *5*, 7050–7059.

(39) Kim, Y. G.; Javier, A.; Baricuatro, J. H.; Torelli, D. A.; Cummins, K. D.; Tsang, C. F.; Hemminger, J. C.; Soriaga, M. P. Surface Reconstruction of Pure-Cu Single-Crystal Electrodes

under CO-Reduction Potentials in Alkaline Solutions: A Study by Seriatim ECSTM-DEMS. *J. Electroanal. Chem.* **2016**, *780*, 290–295.

(40) Schouten, K. J. P.; Qin, Z.; Pérez Gallent, E.; Koper, M. T. M. Two Pathways for the Formation of Ethylene in CO Reduction on Single-Crystal Copper Electrodes. *J. Am. Chem. Soc.* **2012**, *134*, 9864–9867.

(41) Schouten, K. J. P.; Gallent, E. P.; Koper, M. T. M. Structure Sensitivity of the Electrochemical Reduction of Carbon Monoxide on Copper Single Crystals. *ACS Catal.* **2013**, *3*, 1292–1295.

(42) Roberts, F. S.; Kuhl, K. P.; Nilsson, A. Electroreduction of Carbon Monoxide over a Copper Nanocube Catalyst: Surface Structure and pH Dependence on Selectivity. *ChemCatChem* **2016**, *8*, 1119–1124.

(43) Mayrhofer, K. J. J.; Crampton, A. S.; Wiberg, G. K. H.; Arenz, M. Analysis of the Impact of Individual Glass Constituents on Electrocatalysis on Pt Electrodes in Alkaline Solution. *J. Electrochem. Soc.* **2008**, *155*, P78–P81.

(44) Mayrhofer, K. J. J.; Wiberg, G. K. H.; Arenz, M. Impact of Glass Corrosion on the Electrocatalysis on Pt Electrodes in Alkaline Electrolyte. *J. Electrochem. Soc.* **2008**, *155*, P1–P5.

(45) Hori, Y.; Konishi, H.; Futamura, T.; Murata, A.; Koga, O.; Sakurai, H.; Oguma, K. Deactivation of Copper Electrode in Electrochemical Reduction of CO_2. *Electrochim. Acta* **2005**, *50*, 5354–5369.

(46) Wuttig, A.; Surendranath, Y. Impurity Ion Complexation Enhances Carbon Dioxide Reduction Catalysis. *ACS Catal.* **2015**, *5*, 4479–4484.

(47) Subbaraman, R.; Danilovic, N.; Lopes, P. P.; Tripkovic, D.; Strmcnik, D.; Stamenkovic, V. R.;

Markovic, N. M. Origin of Anomalous Activities for Electrocatalysts in Alkaline Electrolytes. *J. Phys. Chem. C* **2012**, *116*, 22231–22237.

(48) Kim, Y. G.; Baricuatro, J. H.; Javier, A.; Gregoire, J. M.; Soriaga, M. P. The Evolution of the Polycrystalline Copper Surface, First to Cu(111) and Then to Cu(100), at a Fixed CO_2RR Potential: A Study by Operando EC-STM. *Langmuir* **2014**, *30*, 15053–15056.